Seismic risk in the Inner Tien-Shan. Lessons from the Suusamyr earthquake.

Alexander Mikolaichuk[1], Jean-Pierre Burg[2], Alexandra Frolova[3], Zoya Kalmetieva[1] and David Fossati[2]

[1] Geodinamic and Hazards Department, Central Asia Institute of Apply Geophysics, Bishkek, Kyrgyz Republic, http://www.caiag.kg
[2] Strukturgeologie, ETH, Zurich, Switzerland, http://www.structuralgeology.ethz.ch
[3] Regional Seismology Department, Institute of Seismology of National Academy of Sciences, Bishkek Kyrgyz Republic, kis@mail.elcat.kg

FNSNF Swiss National Science Foundation
ETH Eidgenössische Technische Hochschule Zürich
Swiss Federal Institute of Technology Zurich
CAGGA Central Asia Geological-Geophysical Association
CAIAG

SUUSAMYR EARTHQUAKE – SURPRISE for the TIEN – SHAN RESEARCHES

It is considered, that though the time-forecast of seismic events is very chancy, places of occurrence are known with a higher degree of probability. The M=7.3 1992 Suusamyr earthquake was unexpected both by inhabitants and by the world scientists because the Inner Tien-Shan was considered to be almost inactive in terms of neotectonic deformation and seismicity (**fig. 2**). The Suusamyr earthquake occurred in an unpopulated region and involved a relatively small number of casualties. However, it weakened the confidence in the reliability of the Tien-Shan seismic hazards assessment. Before this event, many expressed arguments supported the idea of Inner Tien-Shan being a negligible seismogenic area. Arriving against any prediction, this event attracted much international interest. Immediately after earthquake the seismologists and geologists from relevant Institutions of Kyrgyzstan, Kazakhstan, Uzbekistan and Russia have gone to the source area for field investigation. Although several international research teams also visited the earthquake zone during the 2-4 years following the earthquake [Bogachkin et al., 1997; Mellors et al., 1997], competition between these teams prevented the systematic description of active faults in the Suusamyr earthquake zone. Therefore, the seismicity of the Inner Tien-Shan had yet to be specified because the risks remain today under-evaluated. The decision of this problem has not only scientific (informative) content, but the big practical sense. The Suusamyr earthquake has not impaired in big scale, as we have mentioned above already, however, the wrong estimation of seismic danger for the Inner Tien-Shan at the planned construction of the hydroelectric power stations cascade on the Naryn river can threaten to all densely populated Fergana valley. Thanks to the SCOPES-SNSF support (project *No IB7320-110694*) we have done our explorations to gain a reliable understanding of seismic hazards in this region.

We considered:

- the geological structures responsible for earthquakes occurrence;
- definition of the earthquake's maximum magnitude for active faults;
- motion types in the earthquake sources;
- attenuation models.

According to these data we have created a resulting map for a peak ground accelerations at the earthquakes with maximum magnitude.

THE GEOLOGICAL STRUCTURES RESPONSIBLE FOR EARTHQUAKES OCCURRENCE

The area is located to the north-east of the Talas-Fergana (**1**) dextral fault (**see fig. 3**). Two seismoactive fault systems are identified, namely dextral and sinister. All north-west oriented faults (without any exception) are dextral. The Suusamyr-Toluk fault (**5**) is parallel and synthetic to the Talas-Fergana fault. Sublatitudinal striking faults have more complicate history of evolution. It can be seen here both dextral and sinister movements. The Karakol fault (**8**) strikes nearly E-W with evidence for both dextral and sinister movements. Paleomagnetic data on Paleozoic rocks of Central Tien-Shan reveal up to 90° counterclockwise rotation of crustal blocks. This rotation is consistent with sinister movement along the EW fault system during Late Permian –Triass. Dextral movements are recent reactivations. These conclusions are based not only on materials of geological mapping, but also on results of microstructure researches (**fig. 4**).

The analyzed region can be subdivided in the following areas:

- Too-Ashuu Pass Region
- E of Taldy-Bulak
- Ala-Bel Pass Region
- SE of Otmok
- Karakol Pass

To determine the direction and the sense of movement of the fault displacements it was searched appropriate outcrops along the already mapped fault areas. The most difficult part of the work was to find good outcrops. These are unfortunately very rare. The direction and the sense of movement could be determined from striations, slickensides and half-moon structures.

Striations are mostly produced by minerals fibres in fine material along the fault plane. Some striations can also be produced by hard objects driven along the fault surface. The striations give an information about the direction of the movement.

Slickensides are parallel striations on rock surfaces often composed of fibrous crystals that stretch from one side of the fault plane to the other. These are produced by relative motion between opposite sides of fault planes and are commonly associated with brittle faulting [McClay, 1987]. Slickensides form by the progressive crystallization of minerals on the fault surface as the fault slips. When the fault has little steps or irregularities, sliding produces space in which minerals can crystallize. Typical precipitation minerals are calcite, quartz and chlorite. The fibers build on the fault surface steps and can be used to determine the sense of movement. The surface with the fibres moved from the step in the direction where fibres are going. From slickensides outcrops the following data were collected:

- the orientation of the fault surface and the plunge of lineation;
- observations about fault rock, sense of movement from fibers and steps in the fault plane and the nature of fiber growth.

Half-moon structures are structures derived from objects which were pressed and driven along a surface. These moving objects leave a mark on the rock in the direction of movement. By half-moon structures the leading edges show the direction of the removed block. From half-moon structures the following data were collected:

- measured the orientation of the fault surface and the plunge of the leading edges;
- observation records about fault rock and the sense of movement from the leading edges;

The goal of the slickensides and half-moon structure measurements is the evaluation of the orientation of the paleostress tensors. This means the orientation of the principal axes of the stress ellipsoid at the time of faulting.

The evaluation of the paleostress is a statistical computation. This means that the value is an approximation for the faults in a geological significant time and is not a true paleostress tensor. In this sense the term stress is not appropriate because the result is not related to an instantaneous information at one point. However this information is an approximation of the forces which were responsible for the brittle deformation [Burg, 2006].

To evaluate the paleostress tensors we used the Programm FSA 28.3 of Célérier. This program analyses fault and stress tensor data. The input data must include the dip and orientation of the fault plane and the sense and the direction of movement of the faults measured on slickensides or on half-moon structures. The Program uses random stress tensors to evaluate the best tensor for the fault and dip data. The best analytical solutions can then be graphically visualized, which then allows to choose the best solution.

The output sheets show 4 graphics. The graphic in the upper left corner displays all measurements. The graphic in the upper right corner shows the 3 main stresses in form of a pentagon ($\sigma 1$), a square (σ 2) and a triangle (σ 3). The graphic in the centre shows the measured points in a Mohr diagram. To be consistent the measurements must lie between the old failure criteria (the line going through the origin) and the new failure criteria (the upper line). The graph at the bottom shows the angles between the measured bedding and the evaluated stress tensor. This angle should not exceed 30° to correspond to the main stress $\sigma 1$. This means that relevant measurements must lie between 0°-30° and 150°-180°, while the others do not correspond to the main stress [Ghirardello, 2006].

MAXIMAL MAGNITUDE OF THE EARTHQUAKE

For an estimation of the maximum magnitude of earthquake two types of information were used namely the seismostatistical data and data about the paleoseismic dislocations. Unfortunately, in our case the seismostatistical data contain the information only about the Suusamyr earthquake. On figure **2** the map of the M > 4.5 earthquake epicenters, made according to the earthquake catalogue, since the ancient times [Special catalogue …, 1996] is shown. In this catalogue seismic events known under references from the beginning of an A.D. are mentioned. The earthquakes, comparable on magnitude with Suusamyr earthquake, are enumerated here without admissions, at least for last 200-300 years. That is why we involved the data about paleoseismic dislocations [Strom, 2000] for a Mmax definition.

The existing faults associated with the Mmax evaluation were taken as potentially dangerous zones. The largest possible Mmax into the zone contoured by highest isoseismal of the Suusamyr earthquake is 7.7; for South-Aramsu (**6**) and Suusamyr-Toluk (**5**) faults were accepted M= 7.3 and M=6.9 respectively in accordance with magnitudes of the main shock and largest aftershock of the Suusamyr earthquake, which are associated with these faults. Possible magnitudes of M = 8 for the Talas-Fergana Fault (**1**) [Karta seism. Raionirovanya, 1996] and M=7.7 for Northern-Kavak Fault (**3**) were calculated. Along latest one Caldera-like collapses were revealed [Strom, 2000]. According to known laws of relation between scale and a kind of seismodislocations [Solonenko, 1974] and earthquake energy, such phenomena are characteristic for earthquakes with intensity Io= 10-11, i. e. M=7-8.

MOTIONS TYPES IN THE EARTHQUAKES SOURCES

So far as values of peak ground accelerations depend not only on earthquake magnitude, but also from motion type in the source, we have considered the fault plane solutions [E.Book, 1990-2005]. As it was mentioned above already, in source area of Suusamyr earthquake up its occurrence the seismic events did not occur. For this reason we had the fault plane solutions only for the main shock and its aftershocks. Focal mechanisms have been defined by data of polarities for the first motions recorded by the Kyrgyz analogue network. Thus for aftershocks, occurred at first five hours after the main shock, the solutions are not defined owing to the record overlays. The Suusamyr main shock is compressive with a dextral component (**fig. 5**). Focal mechanisms of aftershocks with M ? 4 differ regionally. In the southern area, the thrust component is similar to the motion of the main shock. To the north, thrust components occurred on shallower dipping planes while strike-slip components are important. Normal motions took place in the outskirts parts. The received decisions are well correlated with some definitions of motion types on microstructural researches, for example, for the Too-Ashuu Pass, Ala-Bel Pass and Karakol Pass. As follows from the resulted materials, thrusts and reverses are the prevailing motion types at the faults in boundary of Suusamyr earthquake source area.

For a part of the territory located to the south from source zone of Suusamyr earthquake the strong earthquakes did not occur. So, for a sector of the Talas-Fergana fault only 4 earthquakes with M > 4 have occurred for last 15 years (**fig. 5**). Their focal plane solutions are various and it is impossible to mark out the prevailing motion types. For this reason the fault plane solutions of weaker events with M=3.5 (**fig. 6**) have been involved additionally. It allows make a conclusion about prevalence of strike-slip motion type along the part of the Talas-Fergana fault presented on a map.

Strike-slip motion on the Talas-Fergana Fault (**1**) and thrust motion over the region were used for calculation of seismic hazard.

CREATION OF THE PEAK GROUND ACCELERATION (PGA) MAP

For calculation of peak acceleration values the map has been partition with 0.1 degree steps both on latitude and a longitude. For each node points the peak accelerations expected from all active faults with magnitude and attenuation defined for them were considered. Maximum from all received accelerations values is assigned to the given point. Attenuation is counted according to the correlation (**1**) deduced by Aptikaev F.F. [Aptikaev, Kopnichev, 1979] according to the Tien-Shan earthquakes, and world data. This correlation has the following form:

$$\begin{cases} \lg A = 0.28\,M - 0.8 \lg R + 1.7 + C & A \geq 160 \text{ cm/sek}^2 \\ \lg A = 0.8\,M - 2.3 \lg R + 0.8 & 10 \leq A \leq 160 \text{ cm/sek}^2, \end{cases} \quad (1)$$

where **C** – component is the correction's coefficient to the focal mechanism and is equal 0.2 at reverse motion, 0 - at strike-slip one and - 0.2 - at normal type.

In consideration of rest equal status the reverses are more high-frequency and more dangerous, in comparison with other motion types.

The PGA map was created subject to the prevailing types of focal mechanisms. Local conditions were not considered in this process.

We offer on consideration two PGA maps (**fig. 7** and **8**). At the first case their distinction consists that in a southern part of the research area only North Kavaksky fault is seismoactive that is based by a localization of numerous seismic dispositions [Strom et al., 2008]. At the second case the Ketmentubinsk thrust is also seismoactive so far as according to the generalized geological data the large-scale displacements occurred along this thrust on the quaternary time. As now this geological structure is overlapped (flooded) by the Toktogul reservoir, the given question demands separate detailed study (remote geophysical researches and all-round discussion).

First of all, for a probabilistic estimation of area's seismic hazard it is necessary to define the repeatability's period of possible earthquakes with maximal magnitude. For this purpose it is necessary to calculate the correlation coefficients (**1**), defining the distribution of earthquake's number to its magnitude (Gutenberg-Richter's law). According to the earthquake's catalogue from the ancient times [Spec. Cat. …., 1996] for this area its correlation has the following form:

$$\log (N) = 3.92 - 0.86 Ms, \quad (2)$$

where **N** - number of events in a year. Correlation's coefficient **R** = - 0.95 is for log-linear distribution. This dependence we have taken from the Abdrakhmatov, etc. (2003) reference.

For transition to probabilistic values we used the Poisson law:

$$P = 1 - e^{-t/T}, \quad (3)$$

where **t** is observation's time which is called as a waiting time in prediction problems, **T** - the repeatability period. **P** is a probability to which for this **t** time at least one event will happened with period of repeatability **T**. As usual the prediction is made for 50 or 100 years. In our case we took 50 years as a waiting time, i.e. the **t**. According to (**3**) correlation, if **P**=0.1 then the period of repeatability **T** is equal 475 years. Otherwise, it is possible to say with 10 % probability that for a waiting time of 50 years there will be an earthquake, the period of repeatability of which is equal to 475 years. Magnitude of this maximum earthquake with such period of repeatability we can define from Gutenberg-Richter's (**1**) law, experimentally received for this area since the **N** parameter in this law is depending on the period of repeatability in inverse proportion, i.e. **N=1/T**.

Then from (**1**) **Ms** = 7.7 is the maximum possible magnitude for this area with 10 % - probability of its excess for a waiting time in 50 years.

Thus, for observation's area we have the maximum possible magnitude of 7.7 with the period of repeatability of 475 years and small probability (10 %) of its excess (or 90 % probability of not exceeding value that same) for a waiting time of 50 years.

CONCLUSIONS

So, Suusamyr earthquake appeared completely unexpectedly for all scientific community. Even more unexpected is the conclusion following from our researches: Suusamyr earthquake is far from being strongest one of possible seismic events in the given area. To the south from Suusamyr Earthquake source area seismic danger raises. Seismic hazards in the Inner Tien-Shan are therefore important and Mmax are comparable to those of Northern and Southern Tien-Shan, where numerous destructive events in the XIX and XX centuries have been documented.

Taking into account that on the Naryn river construction of the hydroelectric power stations cascade is planned, seismotectonic researches should become more active in this area.

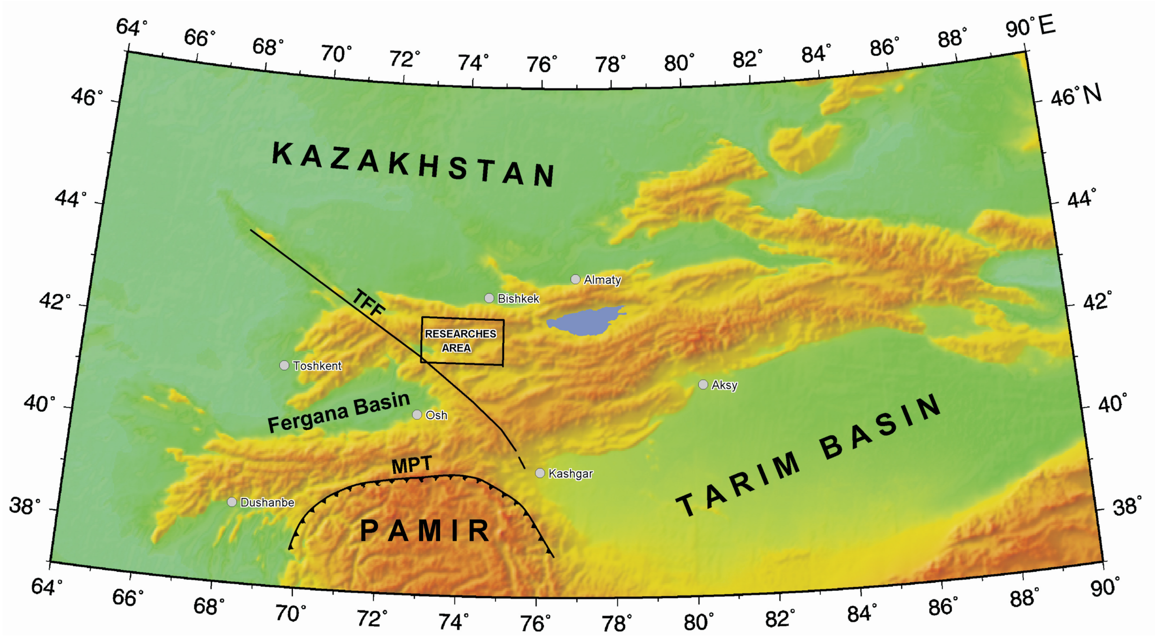

Fig. 1. Overview scheme of the Tien-Shan. TFF – Talas-Fergana Fault; MPT – Main Pamir Thrust

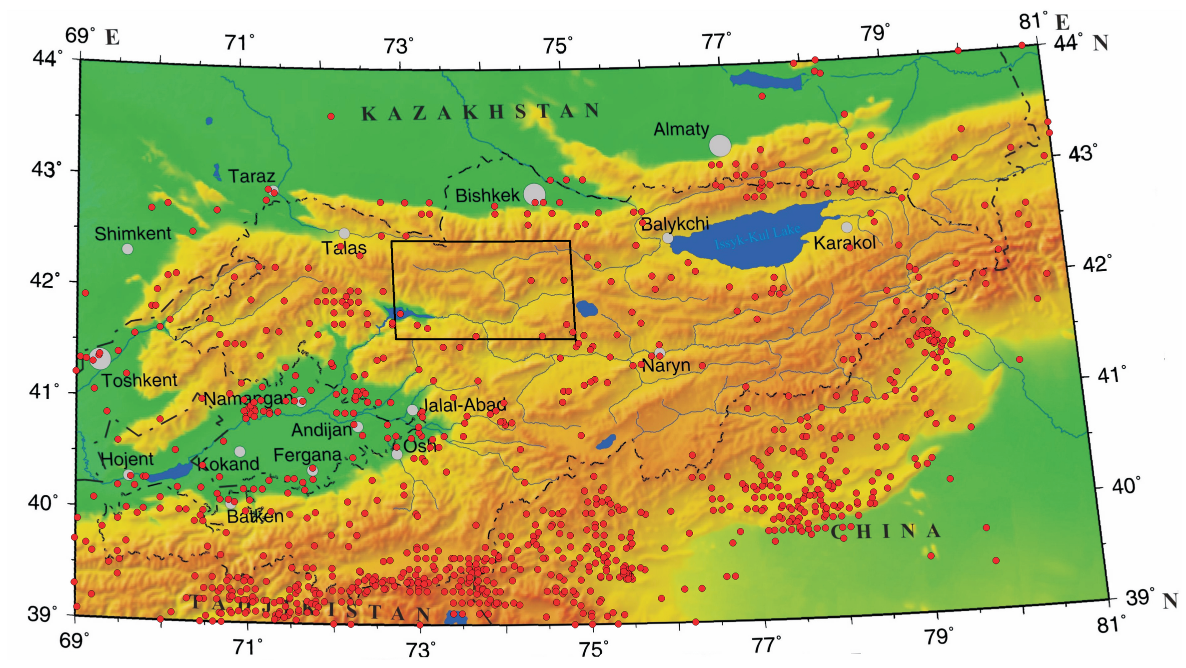

Fig. 2. Map of the earthquakes (M≥ 4.5) epicenters from ancient time till the 1992 M=7.3 Suusamyr earthquake.

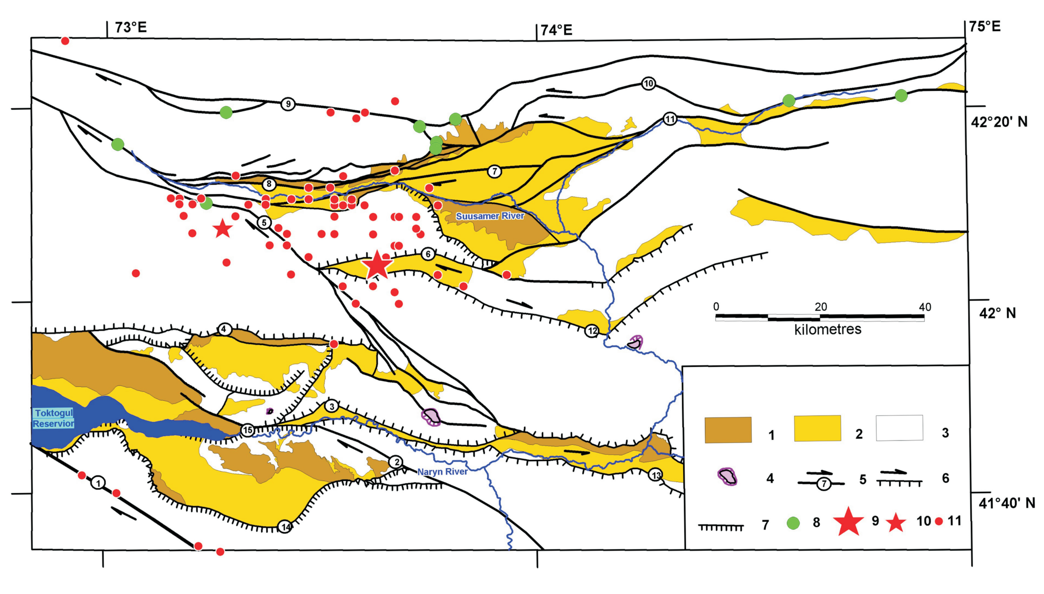

Fig. 3. Neotectonics scheme of the Suusamyr earthquake source area 1 - Upper Pliocene- Lower Pleistocene deposits (Sharpyldak Group), 2 - Mesozoic – Cenozoic deposits, 3 – Paleozoic Formations, 4 – Collapses, rockslides, 5 – Strike-slip faults (names as in text), 6 - Thrust – strike-slip, 7 – Thrust, 8 - Sites of structural-geological observation, 9 - Epicenter of the Suusamyr main shock (M=7.3), 10 - Epicenter of the largest aftershock (M= 6.7), 11 - Epicenters of the aftershocks (M≥3.9)

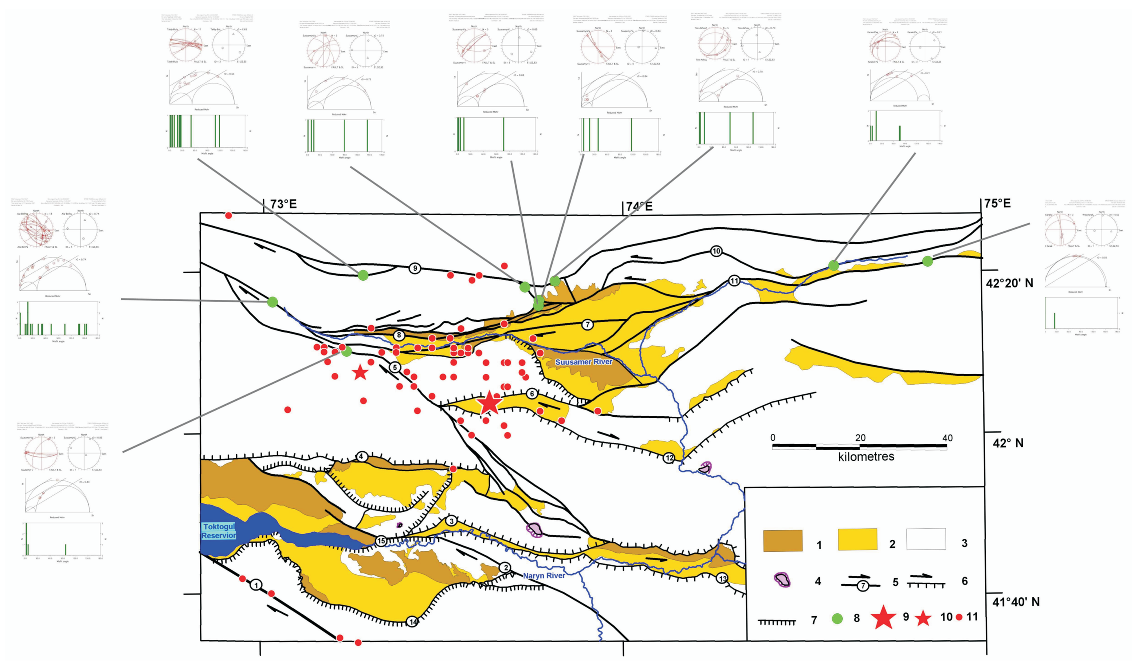

Fig. 4. Analysis graphs of microstructure researches. Legend see on the Fig. 3.

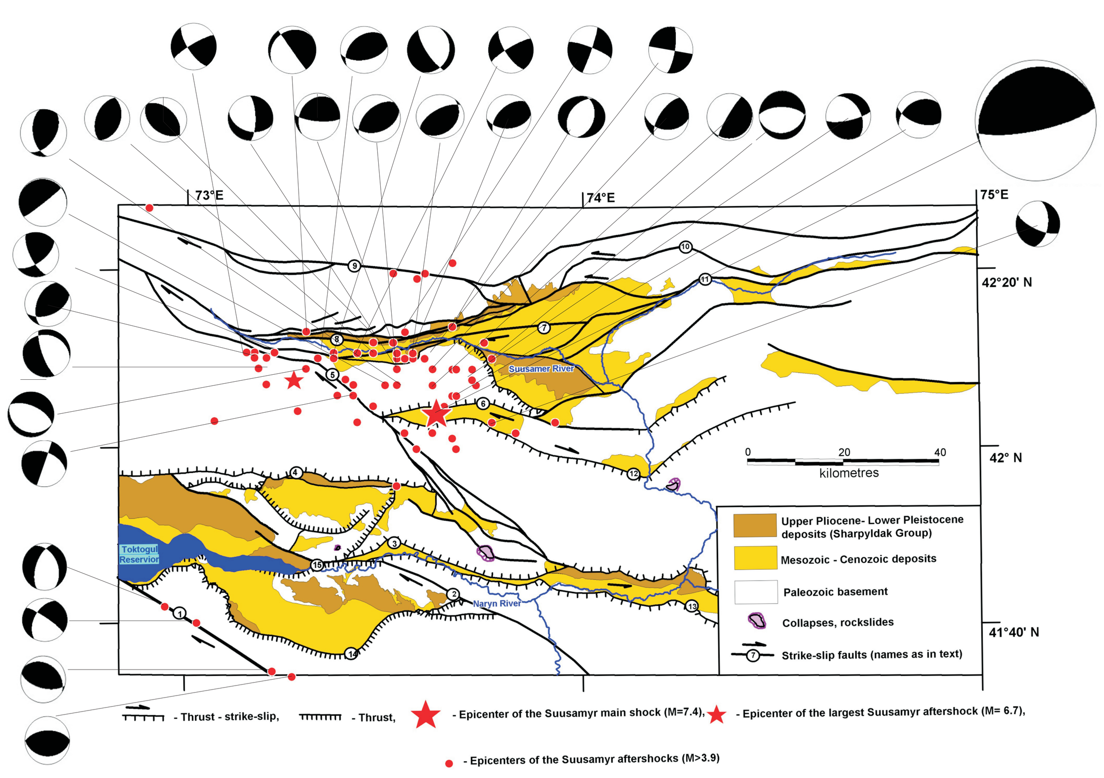

Fig. 5. Map of the earthquakes (M≥ 4.5) sources mechanisms. Largest circle is the Suusamyr earthquake main shock's solution.

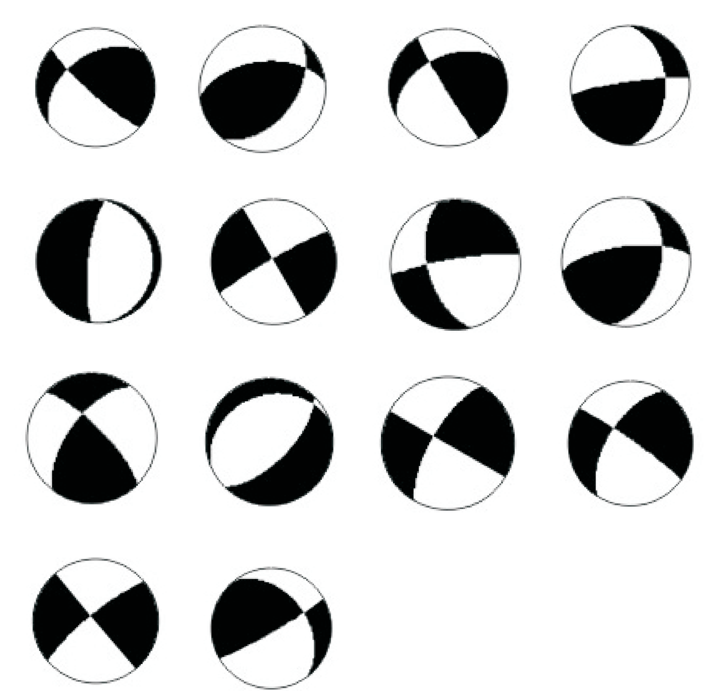

Fig. 6. Motion types for weaker seismic events (M= 3.5) of Talaso-Fergana fault area for 1990-2005.

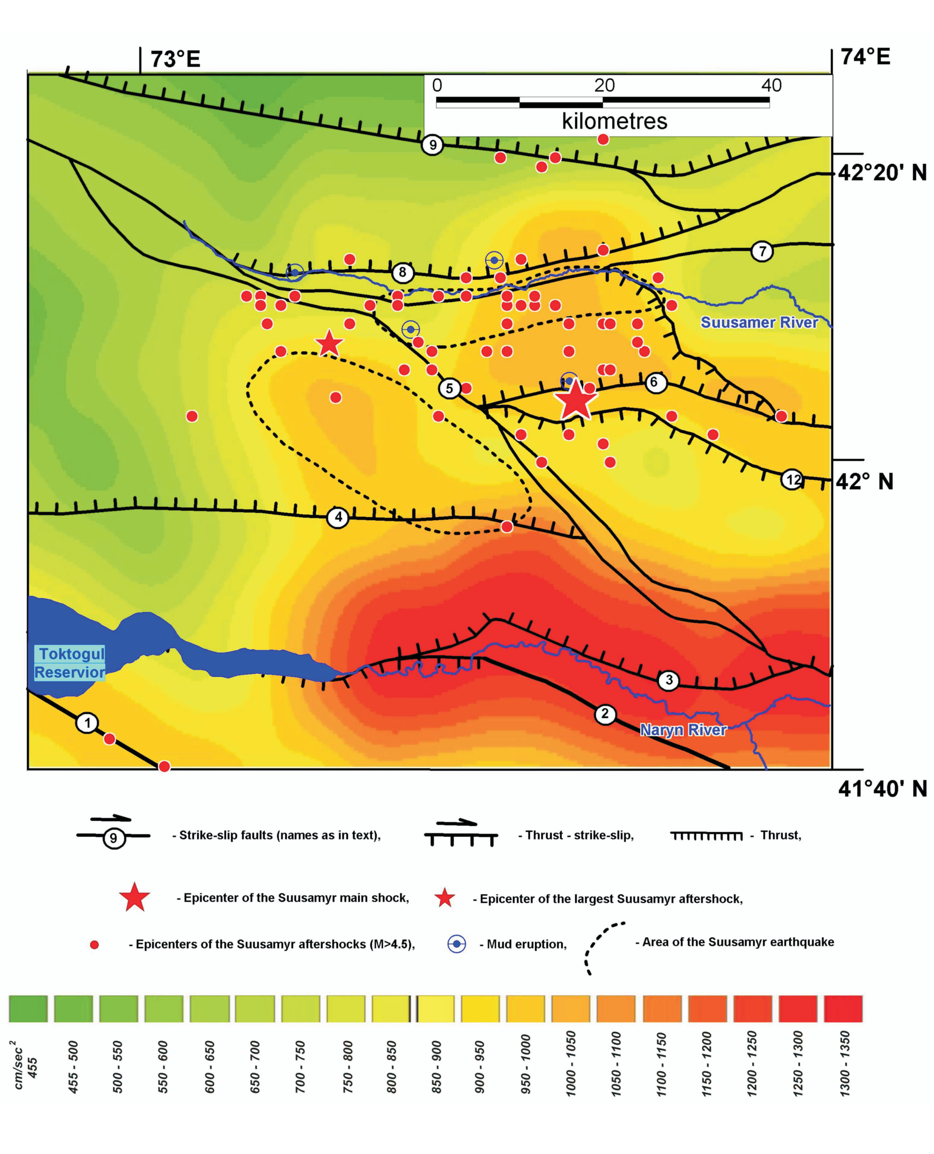

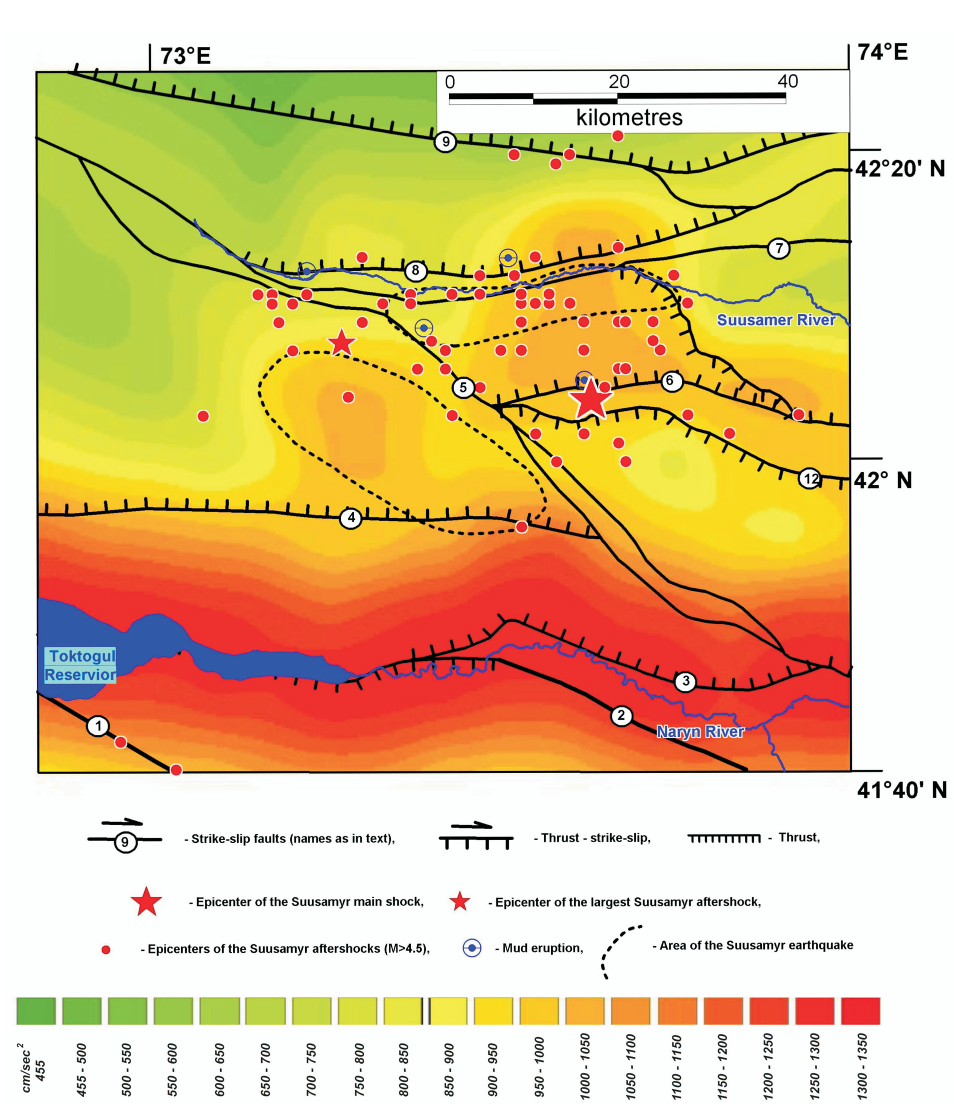

Fig. 7 - 8. Peak Ground Acceleration (PGA) maps of the Inner Tien-Shan including the M=7.3 1992 Suusamyr earthquake source area. The faults names are as on Fig. 3.